Results of Initial Thermal Maturation Modeling of Potential Source Rocks within the Perdido Fold Belt (Alaminos Canyon), Northwestern Deep Gulf of Mexico: Application to Risk Analysis

Joseph C. Fiduk, Independent Geological Consultant

Abstract

One-dimensional, steady state, thermal maturation modeling was conducted at sixteen pseudo-well locations along two profiles in the Perdido fold belt, Alaminos Canyon OCS protraction area. These data are the first published modeling results for strata basinward of the Sigsbee Escarpment. The results give a quantitative evaluation of hydrocarbon generation in this area allowing a more accurate risk assessment.

Geochemical fingerprinting of oil seeps in the Perdido area indicates possible source intervals of Late Jurassic (Tithonian) and Eocene age. The initial results of thermal maturation modeling suggest that Upper Jurassic to middle Eocene strata presently lie within the oil generation window. Other potential source rocks (Oxfordian, Barremian, and Turonian) each lie within the peak oil generation window but at different locations in the fold belt. Possible Eocene source rocks lie within the early oil generation window in the basinward (southeast) half of the fold belt.

Burial history charts for each location relate the timing of source bed maturation to fold belt (trap) formation. Strata within the oil window can vary greatly from fold crest to adjacent syncline. At most locations, the possible Oxfordian source passed through peak oil generation during the Oligocene to Miocene, after fold belt formation. Potential Tithonian, Barremian, and Turonian source rocks did not enter peak oil generation until the Miocene to Present, or have yet to reach peak oil generation on some fold crests. Possible Eocene source rocks have not reached peak oil generation anywhere in the Perdido fold belt. Given the large section within the oil generation window and the specific source intervals that reached peak oil generation after fold belt formation, risk on hydrocarbon generation is considered low.

Introduction

The Perdido fold belt occupies roughly 4000 square km in water depths of 2400-3000 m, within the Alaminos Canyon protraction area, northwestern deep

Paper presented at the AAPG Hedberg Research Conference, "Integration of Geologic Models for Understanding Risk in the Gulf of Mexico," September 20–24, 1998 (Galveston, Texas).

Gulf of Mexico (Fig. 1). This area accounts for the northern one-third of the fold belt; the fold belt extends for at least another 100 km southward into Mexican waters. Over the past thirty years researchers have documented the presence of large northeast-southwest trending structures comprising the fold belt (Bryant et al., 1968; Buffler et al., 1979; Fuqua, 1990, Trudgill et al., 1995a, b). These large fold structures formed in a deformational episode during the Oligocene, between 36-30 Ma, and are interpreted to be salt cored (Trudgill et al., 1999).

Much has been published on the structural aspects of the Perdido fold belt, but only a few published studies deal with other aspects of the Perdido fold belt petroleum systems. Among these studies, Fiduk et al. (1997) presented seismic facies evidence suggesting the possibility of sand-prone siliciclastic deposits within the folded Perdido strata. Aharon et al. (1997) documented the presence of hydrocarbon seeps and chemosynthetic communities on the sea floor above several Perdido folds. From a regional study, Wenger et al. (1994) compiled geochemical data indicating mature Jurassic (Tithonian) and Tertiary (Eocene) source beds across the Perdido fold belt and surrounding area.

The purpose of this paper is to present the preliminary results of one-dimensional (1-D), steady state, thermal maturation modeling of Oxfordian, Tithonian, Barremian, Turonian, and Eocene source beds within the Perdido fold belt. Using the results, a more quantitative assessment of hydrocarbon generation risk can be made for this area than was previously possible. The five chosen intervals were modeled because the Tithonian and Eocene have been sampled in the Perdido area and the Oxfordian, Barremian, and Turonian were considered the intervals next highest in potential. The maturation histories of these five source intervals are compared with published data and the timing of fold belt formation. The comparison assesses the viability of each source as a possible contributor to undiscovered petroleum reserves in the Perdido fold belt.

Data and Methods

The data set for this project consists of sixteen pseudo-well modeling locations arranged along two seismic profiles (Fig. 1). The stratigraphic column (Fig. 2), the fold belt's structural configuration, and the seismic interpretation of the two profiles were taken from our previous work (Trudgill et al., 1995a, b; Fiduk et al., 1997). The only well that penetrates strata of the Perdido fold belt is the Alaminos Canyon 600 well, drilled into the fold belt during 1996. Data from this well were confidential during our thermal modeling study and were not available. Ages assigned to seismic horizons are based on ties to DSDP boreholes 90 and 91, the Atwater Valley 471 well, and the regional deep Gulf basin correlations of Feng (1995) and Feng and Buffler (1996).

Thermal maturation modeling at each of the sixteen pseudo-well locations was performed using the software application BasinMod 1-D. The two seismic profiles were converted to depth and restorations made at 5.5 Ma, 10.5 Ma, 15.5 Ma, 21.5 Ma, 44.5 Ma (Profile A), and 58.5 Ma (Profile B) using the Geosec 2-D restoration software package. Variations through time in autochthonous salt thickness and ocean depth were measured from these restorations. BasinMod automatically calculated other petrophysical parameters needed to compute compaction, porosity, and thermal conductivity as a function of the rock type assigned to each interval. Significant erosional events were found in the pre-fold strata at several locations and were incorporated into the models.

In this initial work, a steady-state heat flow model was used. Present day heat flow was modeled at 43 mW/m^2 following values measured by Nagihara et al. (1996) in the deep Gulf basin. A value of 4°C (39°F) was used for the sea floor water temperature. No sedimentary radiogenic heat was incorporated into the models.

A kinetic model formulated at the Lawrence Livermore National Laboratory was used to derive the thermal maturity of the stratigraphic section (Sweeney and Burnham, 1990). The model calculates vitrinite reflectance (%R_o) values that are used to map the thermal maturity windows of oil (0.6-1.2% R_o), peak oil (0.9-0.95% R_o), wet gas (1.2-2.0% R_o), and dry gas (2.0-2.6% R_o). A standard type II kerogen with its default kinetic parameters was used in all models. Additionally, a sulfur-rich type II kerogen was modeled in the Oxfordian and Tithonian for comparison. Lacking actual measurements, each source interval was assigned a uniform (and conservative) thickness of thirty-three meters (100 ft).

Thermal maturation modeling is dependent on numerous variables, many of which are poorly constrained in the Perdido area. To compensate for this and allow for a reasonable comparison, input variables were made internally consistent between each location (e.g. lithology mix, heat flow, thermal conductivity, heat capacity). Thus, the differences in thermal maturation at each location are interpreted to be real and attributable to their different burial histories (depth of burial, structural uplift, changing thickness of underlying salt). Even with these limitations, the modeling results are the best information for evaluating source bed maturation across the Perdido fold belt and provide the most accurate data for quantifying the risk of hydrocarbon generation.

Discussion

Across the Perdido fold belt, the thermal maturation of potential source beds is primarily influenced by depth of burial and structural uplift, and to a lesser degree by thickness of underlying autochthonous salt. These parameters interact to different degrees at each of the sixteen pseudo-well locations. Two end-member

examples along each profile demonstrate the large range in thermal maturity that exists between the uplifted and deeply buried parts of the fold belt (Figs. 3-4). Maturation windows for all potential source beds, at all locations, are listed in Tables 1 and 2.

Source Maturation

Results from the 1-D thermal maturation modeling were output in two ways: as plots of the burial history and as plots of the source rock history. The burial history charts display the overall timing of sediment burial and uplift at each location. More importantly, they show if or when the five modeled source beds reached various petroleum generation windows based on calculated vitrinite reflectance ($\%R_o$) values (Figs. 3a-b and 4a-b). The source rock history charts show if or when those source beds reached various petroleum generation windows based on calculated kerogen transformation ratios (Figs. 3c-d and 4c-d). The two calculations are based on different parameters and yield different results. Vitrinite reflectance measurements are more common but both methods are used to predict the timing of peak oil generation. In these models, vitrinite reflectance calculations yield a slightly earlier time to early oil generation but a slightly later time to peak oil generation than kerogen transformation calculations.

Similar trends are observed at structurally uplifted locations 2 and 9 (Figs 3a & c and 4a & c) and at the more deeply buried Locations 6 and 15 (Figs. 3b & d and 4b & d). At Locations 2 and 9, the burial history curves are deflected sharply upward by erosion and fold belt formation. Consequently, none of the source beds reach peak oil generation at these locations. On the source rock history plots, transformation curves are deflected sharply to the right indicating a retarding of source maturation by the uplift event. Slightly deeper burial after fold belt formation at Location 9 allowed more of the modeled source beds to reach early oil generation than at Location 2.

At Locations 6 and 15, the burial history curves steepen downward due to fold belt formation (Figs. 3d, 4d). Consequently, all source beds except the Eocene reach peak oil generation at these locations. On the source rock history plots, transformation curves rise sharply indicating a rapid conversion of kerogen to oil because of deeper burial. Transformation curves do not reach the critical moment (peak oil generation) until after folding has started. Thus, each of the sources modeled could have contributed to charging of traps created during fold belt formation.

On each of the source rock history plots (Figs. 3c-d, 4c-d), the possibility of a sulfur-rich Oxfordian and Tithonian source was modeled (dashed lines). A type II-S (sulfur-rich) kerogen employing n-component kinetics calculated from the Monterey Formation (Tissot et al., 1987) was used. The addition of sulfur to the maturation calculation drastically decreases the time necessary for kerogen transformation, all other factors being equal. In the synclines of the Perdido fold

belt (Figs. 3d & 4d), this means a time reduction of 10-15 Ma to reach the critical moment. That would move peak oil generation for the Oxfordian (and possibly the Tithonian) source prior to fold belt formation, jeopardizing its potential to charge later fold structures. Over fold crests, only the Oxfordian source could be jeopardized by this possibility.

Structural Restorations

It is difficult to appreciate the large differences in depth of burial, structural uplift, and thickness of underlying autochthonous salt that affect each location while looking at plan view maps or 1-D plots. Present-day, depth converted sections of Profiles A and B allow the sixteen pseudo-well locations to be viewed in proper perspective (Figs. 5a and 6a). The various petroleum generation windows were posted at each modeling location and connected across the profiles. On these displays, a 2-D perspective of the fold belt is shown and a direct comparison can be made between points as to what part of the section lies within the different petroleum generation windows. Structural restorations at 10.5 Ma, 21.5 Ma, 44.5 Ma (Profile A), and 58.5 Ma (Profile B) allow this perspective to be extended back in time prior to fold belt formation (Figs. 5b-d and 6b-d). The evolution of each source interval at each model location can now be viewed through time across the entire fold belt.

Of the three main parameters influencing thermal maturation, depth to the different petroleum generation windows is mainly controlled by temperature gradient (i.e. depth of burial). Structural uplift has more influence on what part of the section lies within the different petroleum generation windows. On the restorations of Profiles A and B, depth to the different petroleum generation windows changes very little through time (Figs. 5 and 6).

The singular influence of autochthonous salt thickness on source rock maturation cannot be adequately evaluated by these models. Although autochthonous salt thickness changes greatly across both profiles, the depth to any petroleum generation window appears at roughly a constant depth below the sea floor (Figs. 5 and 6). The high thermal conductivity of salt was expected to have a significant effect on thermal maturation where the autochthonous salt was thickest, as modeling of thick autochthonous salt has shown (McBride et al., 1998). But any effect is not readily apparent. Presumably, assumptions made in the steady state model negate some of the salt's influence. However, some thickening of the peak oil generation window does occur where it intersects the top of salt at Locations 3 (Fig. 5c) and 4 (Fig. 5b and c).

Results

Some general observations can be made concerning the modeling results. The inner fold belt (Folds 3-5) has experienced inflation (by salt) through time and is less deeply buried under sediment than the outer fold belt (Folds 1-2). As a consequence, source rocks in the

inner fold belt are less mature than in the outer fold belt. Potential Eocene source rocks have not yet reached oil generation in the inner fold belt. Potential Cretaceous source rocks are mostly in the early oil generation window except at Location 2, where greater uplift has retarded maturation, and Location 11, where the Barremian has reached peak oil generation. Potential Tithonian source rocks have reached peak oil generation only at Location 11 and potential Oxfordian source rocks only at Locations 3, 10, and 11.

In the outer fold belt, potential Eocene source rocks have reached early oil generation in the deeply buried positions between folds at Locations 6, 8, 13, and 15. Potential Cretaceous source rocks have reached peak oil generation in those same positions plus Location 16. Potential Tithonian source rocks have reached late oil generation everywhere except at Location 14 and potential Oxfordian source rocks have reached wet gas generation everywhere except at Locations 7 and 14.

Assessment of Risk

The geologic chance of success for any prospect is found by estimating the probability that four necessary geologic conditions exist. These conditions are the presence of: 1) reservoir rocks, where hydrocarbons can be stored, 2) traps, structural or stratigraphic, 3) hydrocarbon generation and migration into existing traps, and 4) sealing rocks to contain the hydrocarbons in the trap (Rose, 1998). Multiplying these four probabilities together yields the geologic chance of success.

Of the four geologic conditions listed above, our thermal maturation data directly impacts the assessment of hydrocarbon generation. Modeling results shows that the Oxfordian, Tithonian, Barremian, and Turonian type II kerogen source rocks have all reached peak oil generation after the fold belt formed. Eocene type II kerogen source rocks have reached early oil generation. Only an Oxfordian type II-S source rock would have reached peak oil generation prior to fold generation and structural traps being present. Model data indicate that a high probability should be given to the hydrocarbon generation term. The actual value depends on the way individual companies assign probability. The greatest risk should be assigned to the presence of reservoir rock and seal rock.

Confidence in this evaluation could be improved by running multiple steady state models and making reasonable adjustments to input parameters. This would provide a range of maturation results for each potential source bed. Confidence could again be improved by running additional types of models (i.e. transient heat flow or rifting heat flow). This would provide a wider range of maturation results increasing the probability that the actual maturation history falls within the modeled range.

Summary

1. Sixteen 1-D, steady state, thermal maturation models indicate that the main external factors influencing source maturation in the Perdido fold belt are depth of burial and structural uplift. The thickness of underlying autochthonous salt appears not to greatly influence source rock maturation in these models.
2. The minimal influence of salt thickness on thermal maturation is contrary to the findings of other studies. This could indicate that steady state heat flow modeling has underestimated the true thermal maturity of source rocks in the Perdido area.
3. Thermal maturation modeling indicates that potential Oxfordian, Tithonian, Barremian, and Turonian source intervals have all reached peak oil generation at various locations inside the Perdido fold belt. A potential Eocene source has reached early oil generation only in the outer part of the fold belt.
4. With the exception of possible sulfur-rich, Jurassic source rocks, none of the modeled source intervals reached peak oil generation prior to fold belt deformation. This implies that any or all of the modeled source intervals could have contributed to the charging of structural traps found within the Perdido fold belt. Therefore, a low risk to hydrocarbon generation and migration is assigned to the Perdido area.

Acknowledgments

Much of this research was done at the Energy and Minerals Applied Research Center in the Department of Geological Sciences at the University of Colorado. I wish to thank the University and my colleagues Barry McBride, Bruce Trudgill, Mark Rowan, and Paul Weimer for their input to my work. I gratefully acknowledge Platte River Associates, Inc. for the use of their BasinMod 1D software, which served as the basis for this research. I wish to acknowledge Shell Offshore Inc., Texaco Exploration Inc., Amoco Production Company, Mobil Exploration & Producing U.S. Inc., and Western Geophysical who provided seismic data in the Perdido area. I thank Cogniseis Development Company (now Paradigm Geophysical) for the Geosec 2-D software used in the section restorations. I also acknowledge Landmark Graphics Corporation for their software and continuing software support.

References Cited

Aharon, P., H.P. Schwarcz, and H.H. Roberts, 1997, Radiometric dating of submarine hydrocarbon seeps in the Gulf of Mexico: GSA Bulletin, v. 109, p. 568-579.

Baldwin, B. and C.O. Butler, 1985, Compaction curves: AAPG Bulletin, v. 69, p. 622-625.

Bryant, W.R., J. Antoine, M. Ewing, And B. Jones, 1968, Structure of Mexican continental shelf and slope, Gulf of Mexico: AAPG Bulletin, v. 52, p. 1204-1228.

Buffler, R.T., J. Shaub, J.S . Watkins, and J.L. Worzel, 1979, Anatomy of the Mexican Ridges, southwest Gulf of Mexico: AAPG Memoir 29, p. 319-327.

Feng, J., 1995, Post mid-Cretaceous seismic stratigraphy and depositional history, deep Gulf of Mexico: Unpublished Ph.D. thesis, University of Texas at Austin, Austin, Texas, 253 p.

Feng, J., and R. T. Buffler, 1996, Post mid-Cretaceous depositional history, Gulf of Mexico Basin: Structural Framework of the Northern Gulf of Mexico, GCAGS Special Publication in conjunction with Transactions, v.46, p. 9-26.

Fiduk, J.C., P. Weimer, B.D. Trudgill, M.G. Rowan, P.E. Gale, B.E. Korn, R.L. Phair, W.T. Gafford, G.R. Roberts, R.S. Lowe, and T.A. Queffelec, 1997, Seismic Interpretation of Mesozoic-Cenozoic Strata, Perdido Fold Belt Area (Alaminos Canyon), Northwestern Deep Gulf of Mexico: GCAGS Transactions, v. 47, p. 159-168.

Fuqua, D. A., 1990, Seismic structural analysis of the Perdido fold belt, Alaminos Canyon area, northwestern Gulf of Mexico: unpublished Master's thesis, The University of Texas at Austin, Austin, Texas, 89 p.

McBride, B.C., P. Weimer, and M.G. Rowan, 1998, The effect of allochthonous salt on petroleum systems of northern Green Canyon and Ewing Bank areas, northern Gulf of Mexico: AAPG Bulletin, v. 82, p. 1083-1112.

Nagihara, S., J.G. Sclater, J.D. Phillips, E.W. Behrens, T. Lewis, L.A. Lawver, Y. Nakamura, J. Garcia-Abdeslem, and A.E. Maxwell, 1996, Heat flow in the western abyssal plain of the Gulf of Mexico: Implications for thermal evolution of the old oceanic lithosphere: Journal of Geophysical Research, v. 101, p. 2895-2914.

Sweeney, J.J. and A.K. Burnham, 1990, Evaluation of a simple model of vitrinite reflectance based on chemical kinetics: AAPG Bulletin, v. 74, p. 205-244.

Rose, P.R., 1998, Taking the risk out of petroleum exploration-The addoption of systematic risk analysis by oil and gas corporations during the 1990's: AAPG Hedberg Research Conference "Integration of Geologic Models for Understanding Risk in the Gulf of Mexico", program with abstracts, 4 p.

Tissot, B.P., R. Pelet, and Ph. Ungerer, 1987, Thermal history of sedimentary basins, maturation indices, and kinetics of oil and gas generation: AAPG Bulletin, v.71. p. 1445-1466.

Trudgill, B. D., M. G. Rowan, J. C. Fiduk, P. Weimer, P. E. Gale, B. E. Korn, R. L. Phair, W. T. Gafford, G. R Roberts, and S.W. Dobbs, 1999, The Perdido Fold Belt, Northwestern Deep Gulf of Mexico: Part 1. Structural Geometry and Evolution: AAPG Bulletin, v. 83, p. 88-113.

Trudgill, B. D., M. G. Rowan, P. Weimer, J. C. Fiduk, P. E. Gale, B. E. Korn, R. L Phair, W. T. Gafford, J. B.

Dischinger, G. R Roberts, and L. F. Henage, 1995a, The structural geometry and evolution of the salt-related Perdido fold belt, Alaminos Canyon, northwestern deep Gulf of Mexico, in Travis, C. J., B. C. Vendeville, H. Harrison, F. J. Peel, M. R. Hudec and B. F. Perkins, eds., Salt, Sediment and Hydrocarbons: GCSSEPM Foundation, 16th Annual Research Conference, Houston, Texas, p. 275-284.

Trudgill, B. D., J. C. Fiduk, P. Weimer, M. G. Rowan, P. E. Gale, B. E. Korn, R. L. Phair, W. T. Gafford, J. B. Dischinger, G. R. Roberts and L. F. Henage, 1995b, The Geological Evolution of the Deep Water Perdido Foldbelt, Alaminos Canyon, Northwestern Deep Gulf of Mexico, in John, C. J. and M. R. Byrnes, eds., Transactions of the 45th Annual GCAGS Convention, p. 573-579.

Wenger, L.M., L.R. Goodoff, O.P. Gross, S.C. Harrison, and K.C. Hood, 1994, Northern Gulf of Mexico: An integrated approach to source, maturation, and migration, First joint AAPG/AMGP research conference, “Geological Aspects of Petroleum Systems”, 6 p.

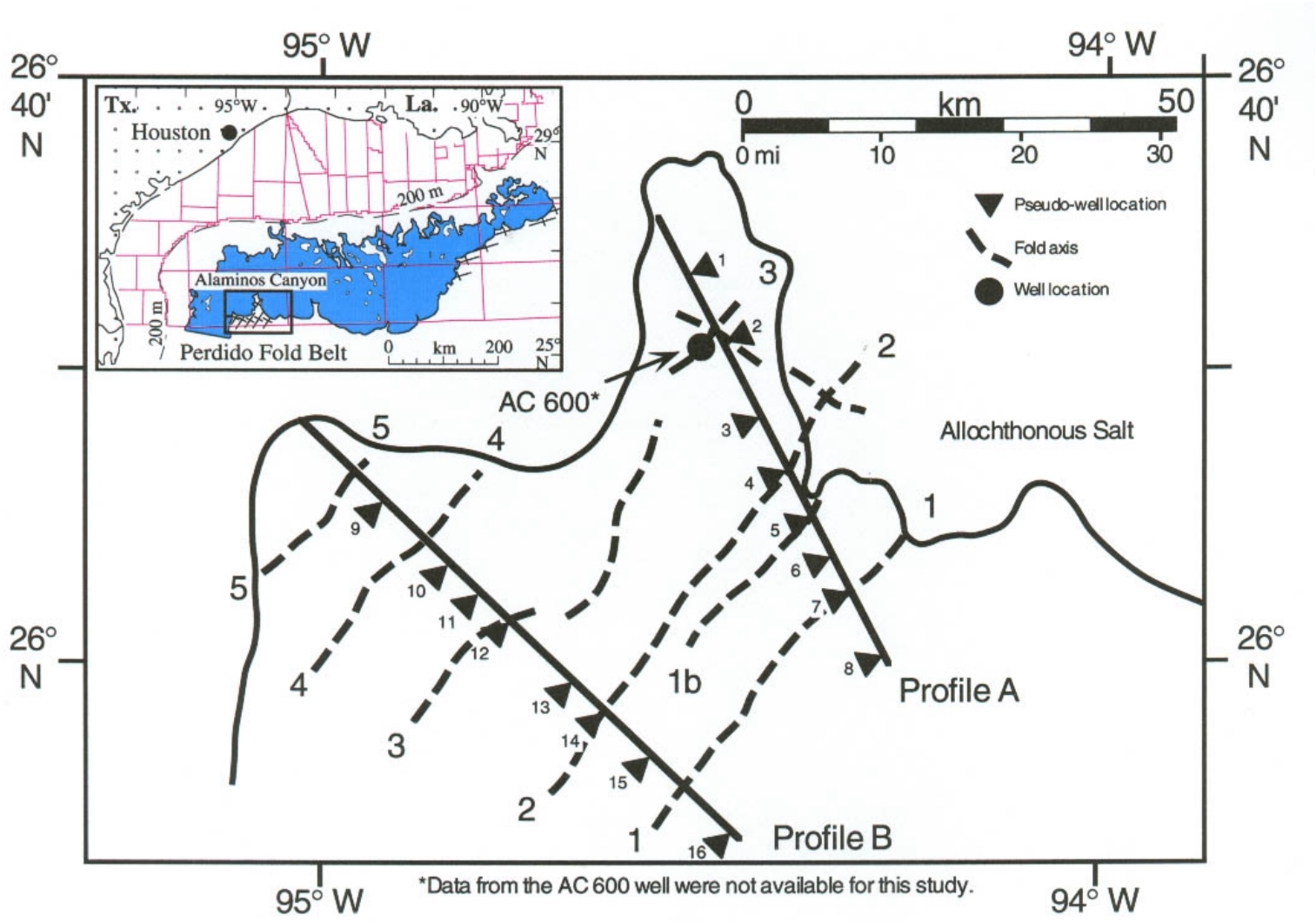

Figure 1. Location map for Perdido fold belt with major fold axes, profile locations, and pseudo-well locations. Inset map shows the northwestern Gulf of Mexico with the location of the Alaminos Canyon OCS area and the Perdido fold belt. The boundaries of major lease (protraction) areas are shown for reference.

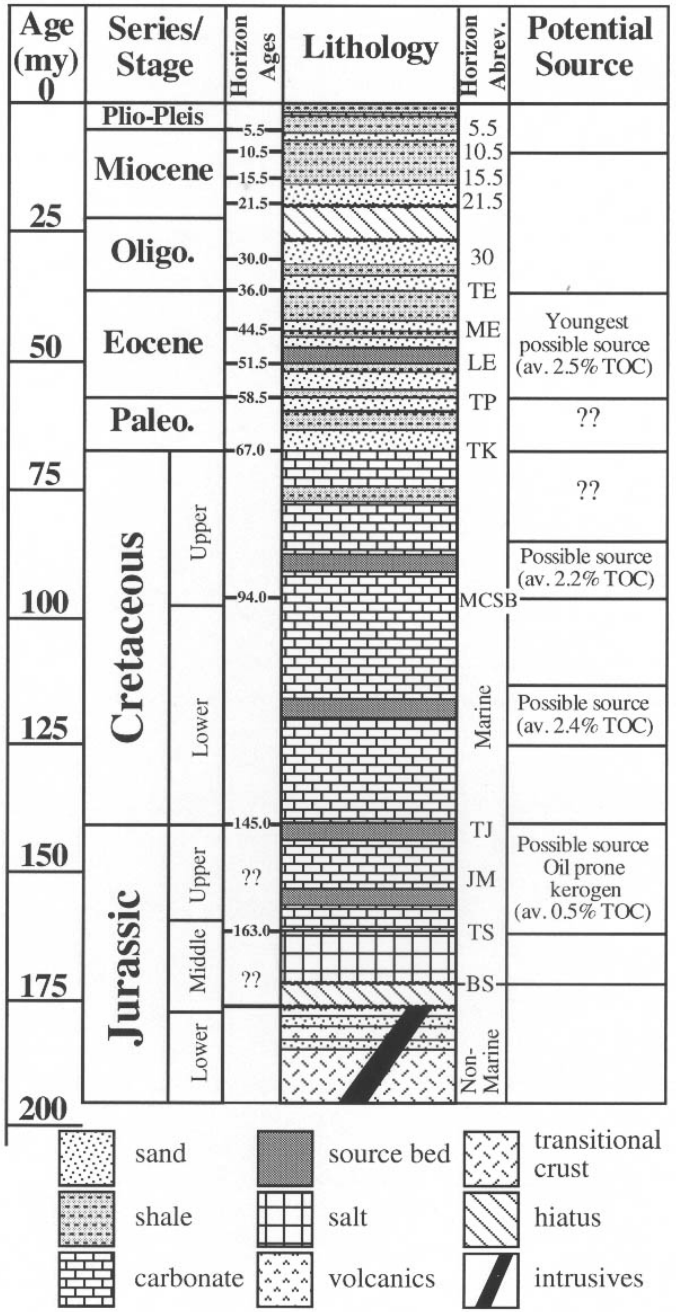

Figure 2. General stratigraphic column for the Perdido fold belt and surrounding area (modified from Trudgill et al., 1995a). The five modeled source intervals from oldest to youngest are: Oxfordian, Tithonian, Barremian, Turonian, and Eocene. Seismic horizons correspond to interpreted horizons in subsequent figures.

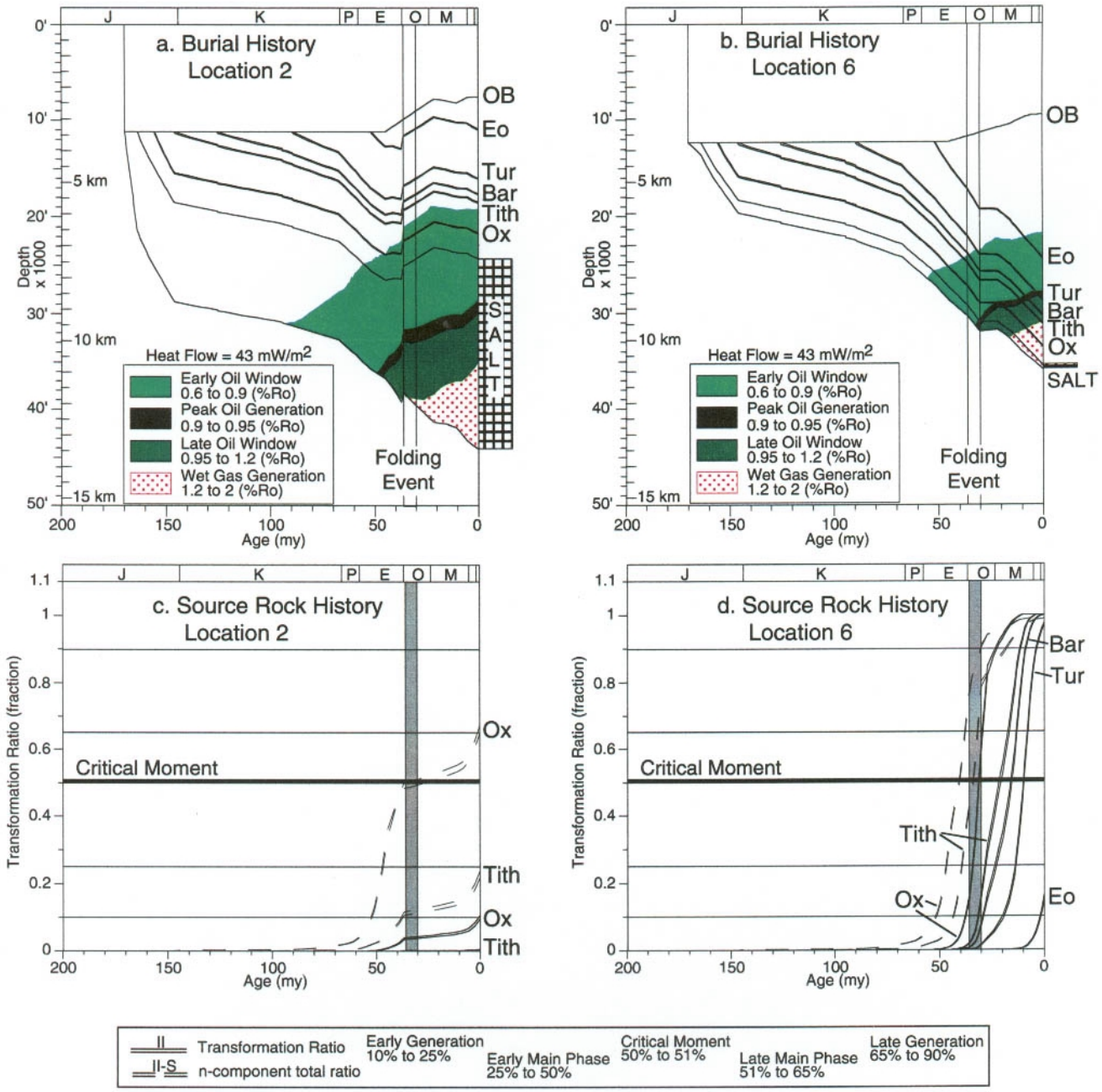

Figure 3. Burial history charts for (a) Location 2, and (b) Location 6, and source rock history charts for (c) Location 2, and (d) Location 6. Dashed lines in (c) and (d) indicate sulfur-rich source modeled. Abbreviations: Ox = Oxfordian, Tith = Tithonian, Bar = Barremian, Tur = Turonian, and Eo = Eocene. Locations shown in Figures 1 and 5.

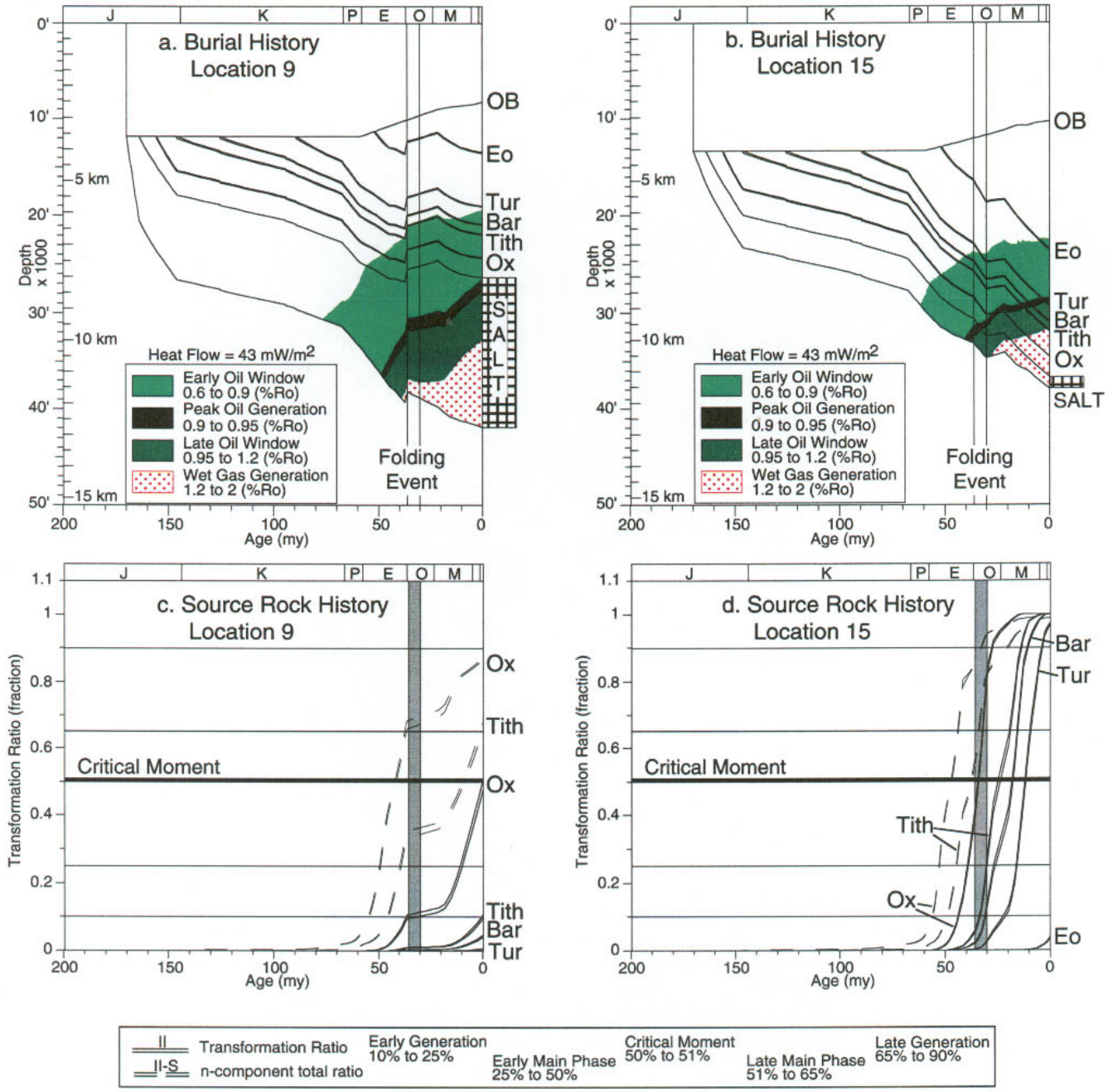

Figure 4. Burial history charts for (a) Location 9, and (b) Location 15, and source rock history charts for (c) Location 9, and (d) Location 15. Abbreviations listed in Figure 3. Locations shown in Figures 1 and 6.

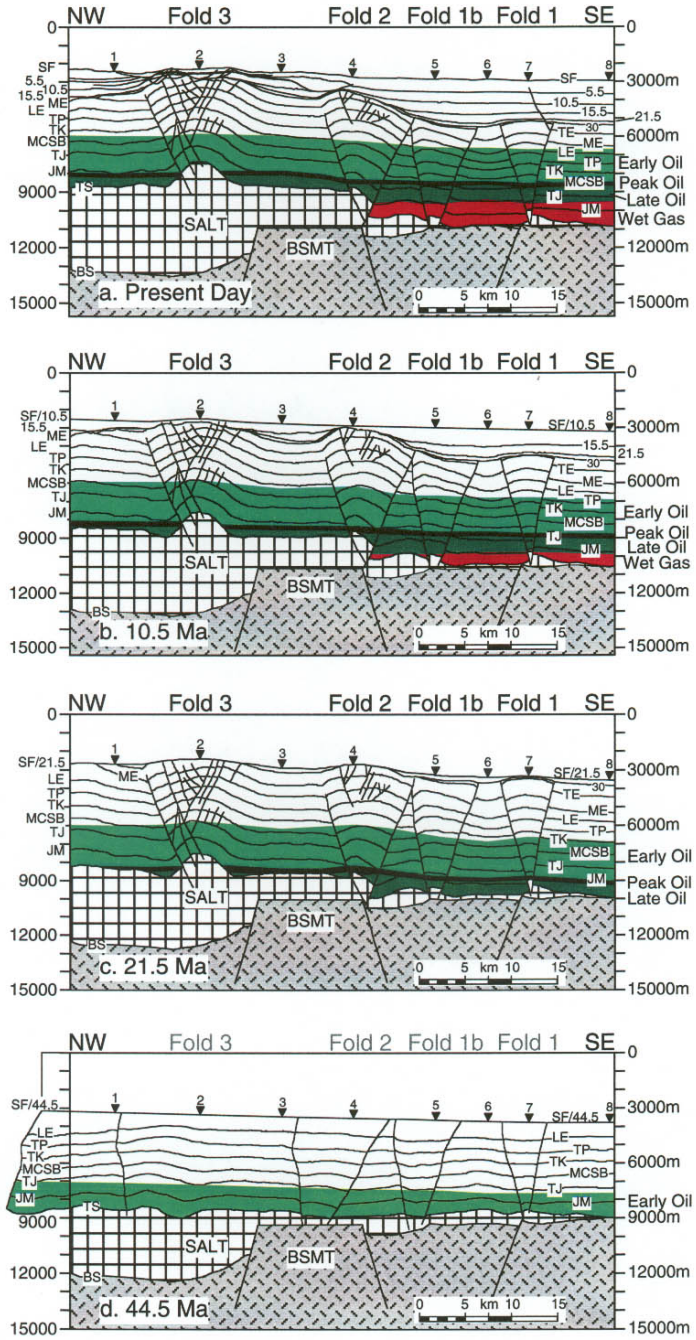

Figure 5. Structural and modeled hydrocarbon generation history for Profile A: (a) depth section; (b) 10.5 Ma restoration; (c) 21.5 Ma restoration; and (d) 44.5 Ma restoration. For all sections the vertical exaggeration = 2:1. Numbered triangles indicate pseudo-well locations. Color code: black = peak oil generation, light green = early oil generation, dark green = late oil generation, red = wet gas generation. Abbreviations: BSMT = Basement, BS = Base Salt, TS = Top Salt, JM = Jurassic Marker, TJ = Top Jurassic, MCSB = Middle Cretaceous sequence boundary, TK = Top Cretaceous, TP = Top Paleocene, LE = Lower Eocene, ME = Middle Eocene, TE = Top Eocene, 30 = 30 Ma sequence boundary, 21.5 = 21.5 Ma sequence boundary, 15.5 = 15.5 Ma sequence boundary, 10.5 = 10.5 Ma sequence boundary, 5.5 = 5.5 Ma sequence boundary, SF = Sea Floor. Profile location shown in Figure 1.

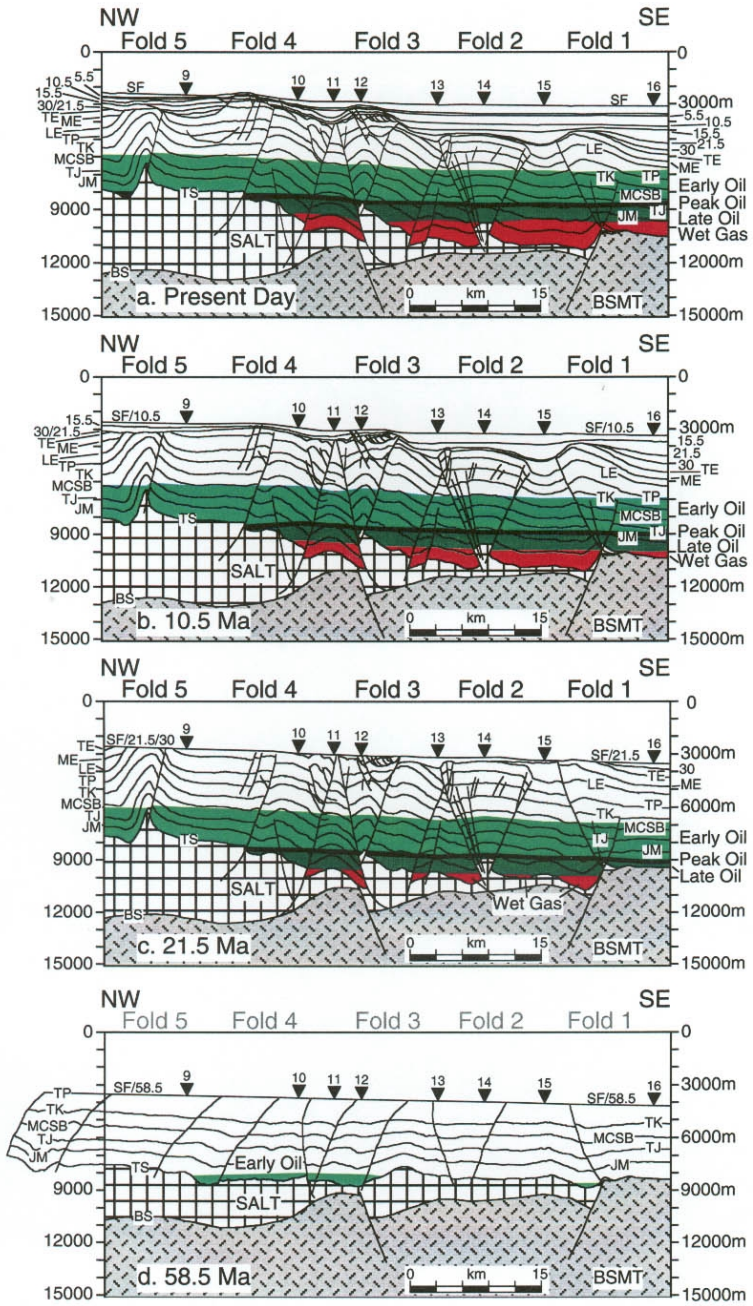

Figure 6. a. Present day depth section for Profile B. b. 10.5 Ma restoration of Profile B. c. 21.5 Ma restoration of Profile B. d. 58.5 Ma restoration of Profile B. For all sections the vertical exaggeration = 2:1. Numbered triangles indicate pseudo-well locations. Color code and abbreviations listed in Figure 5. Profile location shown in Figure 1.

Table 1 Profile A time windows (in Ma) for source bed maturation, steady-state heat flow model. Number spread indicates time when bottom, then top, of interval entered into petroleum generation window. Blank entry means window has not been reached.

Early Oil Gen.	Location 1	Location 2	Location 3	Location 4	Location 5	Location 6	Location 7	Location 8
(%Ro = 0.60)								
Eocene source	----------	----------	----------	----------	----------	8.9-8.5	----------	3.1-2.6
Turonian source	6.0-5.3	----------	16.6-15.2	----------	20.5-19.4	31.2-30.1	24.1-22.4	30.1-29.4
Barremian source	29.2-25.8	----------	34.0-33.3	29.2-21.5	39.6-39.1	35.3-35.0	37.4-36.9	36.5-36.0
Tithonian source	39.6-38.9	----------	38.2-37.6	39.4-39.0	43.3-43.0	37.9-37.5	40.9-40.4	39.8-39.4
Oxfordian source	49.5-49.0	45.2-44.6	48.6-48.2	51.3-50.7	52.1-51.7	45.2-44.8	48.0-47.5	49.7-49.2
Peak Oil Generation (%Ro = 0.90, TR=0.70)								
Turonian source	----------	----------	----------	----------	----------	3.8-3.4	----------	----------
Barremian source	----------	----------	----------	----------	----------	9.0-8.6	----------	5.9-5.4
Tithonian source	----------	----------	----------	----------	2.9-2.5	11.7-11.3	2.6-2.2	9.0-8.6
Oxfordian source	----------	----------	3.9-2.7	----------	13.0-12.4	23.0-22.1	10.0-9.4	22.5-21.5
Critical Moment (Transformation Ratio = 0.50, %Ro = 0.825)								
Turonian source	----------	----------	----------	----------	----------	10.2-9.8	0.6-0.1	6.8-6.4
Barremian source	----------	----------	----------	----------	6.5-6.1	16.2-15.6	6.5-6.1	13.3-12.8
Tithonian source	----------	----------	----------	----------	9.8-9.3	21.8-20.8	9.9-9.4	18.2-17.4
Tithonian IIs	16.7-14.5	----------	30.1-28.9	9.9-8.0	38.6-38.1	34.1-33.8	35.9-35.2	35.2-34.7
Oxfordian source	11.6-10.4	----------	22.7-20.7	7.6-6.4	35.0-31.6	31.5-31.1	25.5-24.0	32.6-32.2
Oxfordian IIs	45.2-44.8	36.4-26.9	43.8-43.4	46.5-46.0	47.6-47.3	40.8-40.4	43.6-43.1	44.9-44.3
Late Oil Generation (%Ro = 0.95)								
Turonian source	----------	----------	----------	----------	----------	1.6-1.1	----------	----------
Barremian source	----------	----------	----------	----------	----------	6.9-6.5	----------	3.7-
Tithonian source	----------	----------	----------	----------	0.6-0.1	9.6-9.2	0.2-	6.7-6.3
Oxfordian source	----------	----------	----------	----------	10.2-9.7	18.5-17.8	7.4-7.0	17.9-17.1
Wet Gas Generation (%Ro = 1.20)								
Tithonian source	----------	----------	----------	----------	----------	0.8-0.3	----------	----------
Oxfordian source	----------	----------	----------	----------	0.7-0.2	8.0-7.6	----------	6.3-5.9

Table 2. Profile B time windows (in Ma) for source bed maturation, steady-state heat flow model. Number spread indicates time when bottom, then top, of interval entered into petroleum generation window. Blank entry means window has not been reached.

Early Oil Gen.	Location 9	Location 10	Location 11	Location 12	Location 13	Location 14	Location 15	Location 16
(%Ro = 0.60)								
Eocene source	----------	----------	----------	----------	6.0-5.4	----------	4.6-4.2	----------
Turonian source	----------	29.0-27.3	33.0-32.7	1.5-0.7	35.6-34.8	21.8-19.9	32.9-32.5	23.4-22.2
Barremian source	13.3-12.3	42.8-42.5	38.5-37.9	28.1-25.0	42.4-42.1	39.0-38.1	39.9-39.4	34.9-34.1
Tithonian source	37.4-35.5	46.3-45.9	42.1-41.6	40.0-39.3	44.0-43.5	42.9-42.4	43.0-42.8	39.4-38.7
Oxfordian source	47.9-47.3	57.1-56.7	48.9-48.6	55.7-55.2	48.8-48.5	52.1-51.7	51.7-51.3	50.3-49.9
Peak Oil Generation (%Ro = 0.90, TR=0.70)								
Turonian source	----------	----------	----------	----------	1.4-0.9	----------	4.2-3.8	----------
Barremian source	----------	----------	5.1-4.4	----------	9.0-8.4	----------	10.9-10.3	3.2-2.8
Tithonian source	----------	----------	10.9-9.9	----------	13.3-12.6	----------	14.2-13.8	5.9-5.4
Oxfordian source	----------	27.4-25.6	29.2-28.8	----------	27.3-26.6	7.7-7.0	27.8-27.2	15.9-15.6
Critical Moment (Transformation Ratio = 0.50, %Ro = 0.825)								
Turonian source	----------	----------	7.8-7.0	----------	11.0-10.4	----------	12.4-11.9	4.9-4.6
Barremian source	----------	----------	23.2-21.9	----------	20.2-19.4	1.0-0.5	18.4-17.8	11.4-10.8
Tithonian source	----------	7.8-5.5	28.2-27.8	----------	25.8-25.0	4.4-3.9	25.1-24.0	14.2-13.8
Tithonian IIs	10.0-8.9	42.0-41.5	36.1-35.6	18.1-16.0	40.6-40.0	35.7-34.6	37.9-37.4	31.8-31.0
Oxfordian source	0.33-	41.6-41.0	33.4-33.1	21.4-18.9	36.6-36.1	29.5-27.7	34.5-34.1	27.7-26.6
Oxfordian IIs	42.5-41.8	52.2-51.6	45.2-44.8	48.9-48.4	46.2-46.0	47.6-47.2	47.3-46.9	46.2-45.7
Late Oil Generation (%Ro = 0.95)								
Turonian source	----------	----------	----------	----------	----------	----------	1.6-1.0	----------
Barremian source	----------	----------	1.4-0.6	----------	6.1-5.4	----------	8.1-7.6	0.5-
Tithonian source	----------	----------	6.2-5.4	----------	10.1-9.5	----------	11.9-11.4	3.8-3.3
Oxfordian source	----------	16.2-14.0	26.9-26.1	----------	23.6-22.8	4.4-3.8	23.3-22.2	14.0-13.6
Wet Gas Generation (%Ro = 1.20)								
Tithonian source	----------	----------	----------	----------	----------	----------	0.9-0.3	----------
Oxfordian source	----------	----------	4.4-3.6	----------	8.3-7.7	----------	10.9-10.4	3.4-2.9